

Article

# A Template-Free Microwave Synthesis of One-Dimensional Cu<sub>2</sub>O Nanowires with Desired Photocatalytic Property

Rui Chen <sup>1</sup>, Zuoshan Wang <sup>1</sup>, Qingqing Zhou <sup>1</sup>, Juan Lu <sup>1</sup> and Min Zheng <sup>2,\*</sup>

<sup>1</sup> College of Chemistry, Chemical Engineering and Materials Science, Soochow University, Soochow 215123, China; 20164209195@stu.suda.edu.cn (R.C.); zuoshanwang@suda.edu.cn (Z.W.); qqzhou@stu.suda.edu.cn (Q.Z.); lujuan@suda.edu.cn (J.L.)

<sup>2</sup> College of Textile and Clothing Engineering, Soochow University, Soochow 215123, China

\* Correspondence: zhengmin@suda.edu.cn; Tel./Fax: +86-0512-8518-7680

Received: 27 July 2018; Accepted: 19 September 2018; Published: 27 September 2018



**Abstract:** One-dimensional Cu<sub>2</sub>O nanowires were successfully prepared with a template-free microwave synthesis. Neither a surfactant was needed (to induce the growth), nor a long reaction time was required for this method. The structural investigation confirmed the successful preparation of Cu<sub>2</sub>O. The morphology images showed that the radial size of the Cu<sub>2</sub>O nanowires was 10 nm. The possible growth mechanism was hypothesized according to morphology evolution and references. A series of time-dependent experiments indicated that as time increased, Cu<sub>2</sub>O primary particles grew radially into nanowires under microwave energy irradiation. The condition-variable tests revealed that the suitable quantity of NaOH played a vital role in Cu<sub>2</sub>O nanowire formation. The photocatalytic property of the sample was investigated by degradation of methyl orange under the irradiation of visible light at room temperature. Benefiting from its unique large surface area, 4 mg of the prepared catalyst degraded 73% of methyl orange (10 mg L<sup>-1</sup>) in 120 min.

**Keywords:** One-dimensional Cu<sub>2</sub>O nanowires; microwave synthesis; growth mechanism

## 1. Introduction

Cu<sub>2</sub>O is a typical narrow bandgap p-type semiconductor, and its band gap is 2.0–2.2 eV [1]. The narrow band structure enables Cu<sub>2</sub>O to utilize visible solar light, the main solar irradiation scattered on the ground. In particular, the electrons on the valence band are excited by visible-light energy to the conduction band, producing active carriers [2]. In this process, the Cu<sub>2</sub>O semiconductor converts the “green” light energy into electronic energy. As a consequence, Cu<sub>2</sub>O is widely studied for its photocatalytic ability, be it either decomposing water into H<sub>2</sub> or degrading organic pollutants [2–6]. Cu<sub>2</sub>O is also applied in antibacterial applications [7–9], in battery electrodes [10–12], and sensors [13–15] due to its abundance, nontoxicity, and low cost [16].

One-dimensional semiconductor materials with many advantages, such as lower material consumption, efficient coupling with sunlight, effective light-to-electricity conversion capabilities, and drastically different physicochemical behaviors from bulk materials have been reported for photovoltaic applications [17–19]. Therefore, the synthesis of one-dimensional Cu<sub>2</sub>O is widely studied, with methods such as electrodeposition [20], liquid phase reducing method [21], oxidation method [22] and solvothermal method [23] all being explored. Usually, either a sacrificial hard template (such as a Cu grid) is required to orientate well-aligned Cu<sub>2</sub>O nanowire arrays [24–26], or a surfactant soft template (such as sodium dodecyl, o-anisidine, pyrrole, or 2,5-dimethoxyaniline) is needed to guide the radical growth of Cu<sub>2</sub>O [27,28]. Although there is a challenge to achieve the template-free synthesis to form 1D Cu<sub>2</sub>O, a polyol method was recently found to synthesize Cu<sub>2</sub>O nanowire without any

template [19]. By only using a precursor of copper acetate and ethylene glycol/diethylene glycol or polyethylene glycol, Cu<sub>2</sub>O nanowire can be formed in hours [29–31], in which the polyol is not only applied as the solution but also as a reactant.

Compared with the traditional heating method, microwave irradiation synthesis was reported to possess advantages such as volumetric heating, fast kinetics, homogeneity, selectivity, less energy consumption, and time-saving benefits [32,33]. As a “green” synthesis technique, microwave irradiation is currently paid wide attention for controlling the morphologies of inorganic nanoparticles, including Cu<sub>2</sub>O nanoparticles [32,34–38]. This is because key parameters of a microwave system such as power inputs and heating frequency are expected to have great influence on the structure [39]. However, Cu<sub>2</sub>O nanowires have been scarcely synthesized with a microwave-assisted method. Herein, we apply the microwave-assisted route, combined with the polyol method, to form Cu<sub>2</sub>O nanowires. This synthesis needs no template, strict experimental conditions, or long duration. In this process, ethylene glycol was chosen as reducing agent and solution agent, copper acetate as copper source, sodium hydroxide as a precipitator, and small-size Cu<sub>2</sub>O nanowires were fabricated in minutes without any template.

## 2. Experiment

### 2.1. Materials

Copper acetate (Cu(Ac)<sub>2</sub>H<sub>2</sub>O), sodium hydroxide (NaOH), polyvinyl pyrrolidone (PVP K-30), and ethylene glycol (EG) were purchased from Shanghai Chemical reagent Co., Ltd. (Shanghai, China). All the chemicals were analytical reagents and used as received without further purification and deionized water was used throughout this work.

### 2.2. Preparation

Cu<sub>2</sub>O nanowires were synthesized in a facile microwave-assisted route. The detailed process is as follows: 2 mL 0.1 M Cu(Ac)<sub>2</sub> was dispersed into 50 mL EG, together with 0.4 g PVP K-30 as a dispersion agent. Then, 2 mL 0.2 M NaOH solution was added dropwise under magnetic stirring. After stirring for a period, the precursor was transferred into a 100 mL three-necked flask for the microwave process.

For the microwave procedure, the microreactor (XH-100B) was obtained from Beijing Xianghu Technology Development Co. Ltd. (Beijing, China). The above precursor was treated for 8 min with a power of 800 W under microwave energy. Finally, the resulting precipitation was separated through centrifugation and was washed several times by deionized water and ethyl alcohol.

### 2.3. Characterization of the Samples

Crystal structures of the samples were characterized with X-ray diffraction (XRD) on a X' Pert-Pro MPD X-ray diffractometer (Panalytical, Almelo, Holland) with Cu-K $\alpha$  radiation ( $\lambda = 0.154$  nm), scanning from 20° to 80° with a scanning voltage of 40 kV and a scanning current of 100 mA. The prepared powder sample was flattened into the groove of the glass sheet for the XRD test. XRD data were analyzed by the software, Jade (6.0, Materials Data, Inc., New York, NY, USA). Morphology of the samples was observed with transmission electron microscopy (TEM, FEI TecnaiF20, FEI, Hillsboro, AL, USA), scanning electron microscopy (SEM, Hitachi S-4700, Hitachi Limited, Tokyo, Japan) and high-resolution transmission electron microscopy (HRTEM, TecnaiG20, FEI, Hillsboro, AL, USA). The product dispersive ethanol solution was dropped on a silicon slice and dried for SEM test. The product dispersive ethanol solution was dropped on a carbon-film copper network for the TEM test. TEM images and Selected Area Electron Diffraction (SAED) patterns were captured by the testing machine, and analyzed by the software Digital Micrograph (3.7.4, Gatan Inc., New York, NY, USA). Their chemical compositions were investigated with energy dispersive X-ray

spectroscopy (EDX, Thermo Fisher Scientific, Shanghai, China). Surface area and pore size distribution analyses were taken by Brunauer-Emmett-Teller (BET) method with a Micromeritics Tristar 3020.

#### 2.4. Photocatalytic Activity

Photocatalytic evaluations of the prepared one-dimensional Cu<sub>2</sub>O nanowires were performed in a photochemical reaction instrument (XuJiang Electromechanical Plant, Nanjing, China) to degrade methyl orange dye (MO) under visible light irradiation at room temperature. A 500 W xenon lamp (XuJiang Electromechanical Plant, Nanjing, China) equipped with a UV filter ( $\lambda > 420$  nm) was employed as the irradiation source. The procedure was described as follows: 4 mg of the as-made samples were dispersed into 100 mL MO solution (10 mg L<sup>-1</sup>) under ultrasonic vibration for 5 min. With water flowing around the lamp to keep the temperature steady between 20 and 25 °C, the suspension system was irradiated for 90 min. Once the irradiation commenced, 4 mL of the suspension was taken out to remove precipitation at every specific interval.

A trapping experiment of the active species was done by adding triethanolamine (TEOA) (5 mM), isopropanol (IPA), and ascorbic acid (L-AA) to the MO solution as scavengers of h<sup>+</sup>, ·OH, and ·O<sub>2</sub><sup>-</sup>, respectively. The concentration of MO was tested after visible light illumination for 120 min.

### 3. Results and Discussion

#### 3.1. Structure and Morphology

In order to confirm the phase composition of the prepared sample, the structure was characterized by XRD analysis, see Figure 1A. The diffraction peaks with 2 $\theta$  value of 29.5°, 36.4°, 42.3°, 61.5°, 73.6°, and 77.8° corresponded to the (110), (111), (200), (220), (311), and (222) crystal planes of the face-centered cubic Cu<sub>2</sub>O phase, respectively. The space group was Pn-3m (224), a = 4.270, b = 4.270, and c = 4.270, (JCPDS#99-0041). To further validate the composition of the prepared samples, the element distribution of the sample was checked by EDS analysis, see Figure 1B. As the graph showed, the sample included two elements, Cu and O. In particular, the peak at around 2.2 keV belonged to Au, sprayed onto the sample to increase the conductivity, and the weak peak to the left of the O peak belonged to adventitious carbon from the sample preparation or the EDS instrument itself [40].

The HRTEM investigation, see Figure 1C, confirmed that the basal spacings of nanowires was 2.4 Å and 2.1 Å, which were consistent with the spacing of the (111) and (200) crystal plane of Cu<sub>2</sub>O (JCPDS#99-0041). In the selected-area electron diffraction image, see Figure 1D, four diffraction rings with lattice features corresponded to the (200), (111), (220), and (311) planes. Figure 1C also revealed that the prepared Cu<sub>2</sub>O nanowire was not composed of radially-grown mono-crystal but was constituted by aggregates of nanocrystals, which were around 5 nm in diameter. In conclusion, the above analyses supported each other and confirmed the successful preparation of the Cu<sub>2</sub>O crystalline structure.

To further investigate the morphologies and microstructures of the as-prepared samples, SEM and TEM images of different magnifications were taken. As shown in Figure 2, the prepared Cu<sub>2</sub>O appeared to have a one-dimensional nanowire structure, of which the diameter was around 10 nm. The nanowires cross and overlap each other with large slits in between. The high-resolution image showed the nanowires were well-arranged.

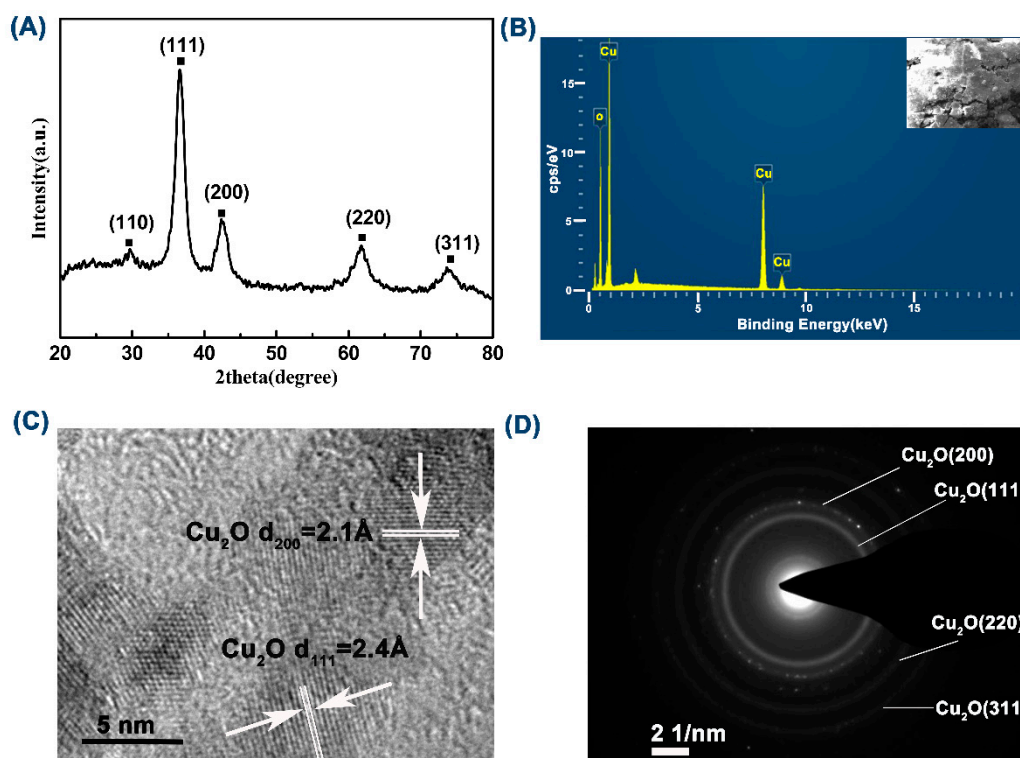


**Figure 1.** (A) X-ray diffraction (XRD) pattern of the prepared  $\text{Cu}_2\text{O}$ ; (B) EDX map of the prepared  $\text{Cu}_2\text{O}$ ; (C) high-resolution transmission electron microscopy (HRTEM) image of the prepared  $\text{Cu}_2\text{O}$ ; (D) selected area electron diffraction image of the prepared  $\text{Cu}_2\text{O}$ .

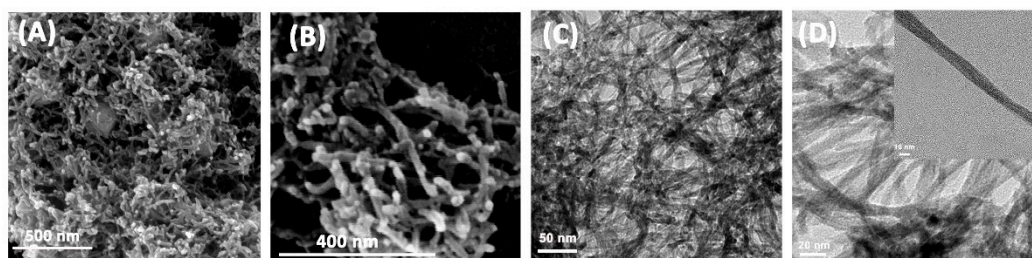


**Figure 2.** Scanning electron microscopy (SEM) (A,B) and transmission electron microscopy (TEM) (C,D) images of the prepared  $\text{Cu}_2\text{O}$  one-dimensional nanowires.

Compared with bulk material, one-dimensional material tends to possess a larger surface area. To characterize the surface area of the product, nitrogen absorption-desorption isotherms, see Figure 3A, were tested using the Brunauer-Emmett-Teller (BET) method, which suggested the specific surface area of the prepared one-dimensional  $\text{Cu}_2\text{O}$  nanowires was  $99.98 \text{ m}^2 \text{ g}^{-1}$ . As shown in Figure 3A, the prepared one-dimensional  $\text{Cu}_2\text{O}$  exhibits type-IV isotherms with H3-type hysteresis loops. The absorption isotherm rose abruptly under high pressure (0.9–1.0) due to mass capillary condensation. An H3-type hysteresis loop suggested that most pores are large mesopores or macropores, attributed to the slits among the nanowires. Large surface areas provide more active sites for photocatalysis. The pore size distribution of the samples was also obtained from the Barret-Joyner-Halenda (BJH) desorption isotherm. As Figure 3B shows, the sample displayed a major large mesopores and macropores distribution, which was in accordance with the absorption-desorption isotherms.

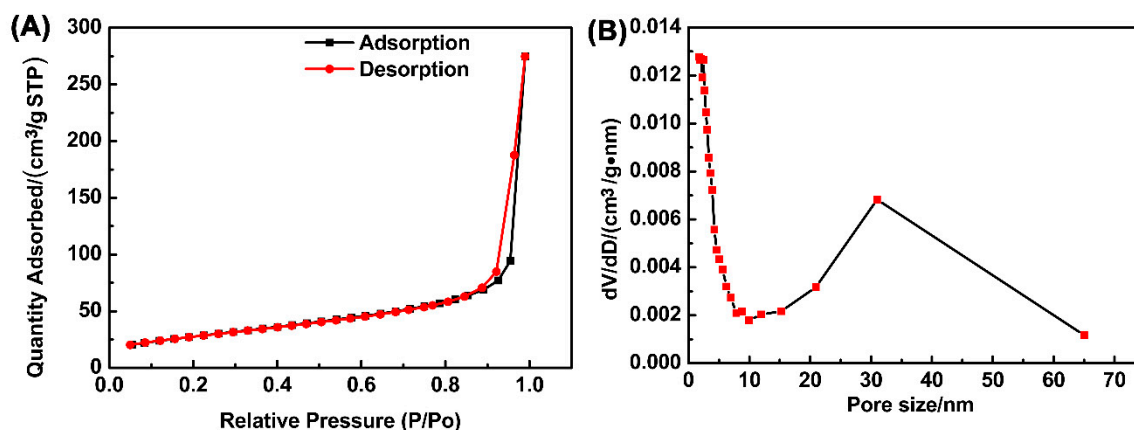
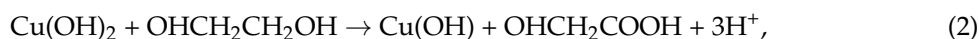


Figure 3. Nitrogen adsorption-desorption isotherms of Cu<sub>2</sub>O (A); Pore size distributions of Cu<sub>2</sub>O (B).

### 3.2. The Mechanism Analysis

To make the influence of each component on the Cu<sub>2</sub>O nanowire clear, control experiments were performed. It was found that the morphology of the product is influenced greatly by the quantity of sodium hydroxide. Firstly, moving NaOH out of this system, there was no precipitate after the microwave process, so NaOH worked as the precipitate agent as in the other reported Cu<sub>2</sub>O synthesis [36,38,41]. According to the report, Cu(OH)<sub>2</sub> is promoted as soon as NaOH is added into the reaction medium, so the quantity of NaOH in the preparation influences the morphology of metallic oxides in some way. In this experiment, the morphology of Cu<sub>2</sub>O turned from one-dimensional nanowires into three-dimensional bulk when the Cu<sup>2+</sup>/2OH<sup>-</sup> ratio surpassed 1:1 to 2:3, see Figure 4B, and 1:2, see Figure 4C, in this process. In fact, it was observed that Cu<sub>2</sub>O nanowires tend to agglomerate into bulk as long as the Cu<sup>2+</sup>/2OH<sup>-</sup> ratio surpassed 1:1. Thus, the quantity of NaOH played a key factor in this process. Secondly, getting rid of PVP, the TEM image indicated that the morphology of the sample was also a one-dimensional material but in severe aggregation, see Figure 4A. As a result, PVP was supposed to work as the dispersing agent, which restricted the particles from aggregation in this preparation, although it was often used to induce the growth of one-dimensional materials [21]. EG played three roles in this system. First, it worked as a solvent, which owns a comparatively high loss tangent (1.17) [42] and can couple with the microwave energy more efficiently. Second, it acted as a reductant. Third, it promoted the formation of small-sized 1D Cu<sub>2</sub>O by modifying the mobility of the primary particles in suspension as well as its effective collision rates [42].

In order to figure out the growth process of the one-dimensional Cu<sub>2</sub>O nanowires, TEM images of samples at different reaction times (2, 4, and 6 min) were taken, see Figure 4D–G. It could be observed that as time increased, Cu<sub>2</sub>O primary particles disappeared, then grew into nanowires in an orderly fashion. The possible reaction process is described as follows:





### 3.3. Photocatalytic Activity

The degradation of MO was investigated as a model reaction to evaluate the photocatalytic activity of synthesized catalysts under visible light ( $420 \text{ nm} < \lambda < 780 \text{ nm}$ ) irradiation. The degradation rate was calculated according to the following formula:  $\eta = C/C_0^{-1}$ , where  $C$  and  $C_0$  stand for reaction and initial concentrations of MO. As Figure 6A showed, the prepared one-dimensional  $\text{Cu}_2\text{O}$  nanowires removed 73% of the MO in 120 min. A dark experiment of prepared one-dimensional  $\text{Cu}_2\text{O}$  nanowires was also done to determine the amount of absorption from degradation. Figure 6A suggested that in dark experiments, only 14% of the MO was absorbed, which confirmed the effect of photocatalysis. The blank experiment showed that, without the addition of a photocatalyst, MO dye molecule could not be degraded under visible light irradiation. All in all, most of the dyestuff was decomposed by prepared one-dimensional  $\text{Cu}_2\text{O}$  nanowires under visible light irradiation for 120 min with only 4 mg of the prepared catalyst.

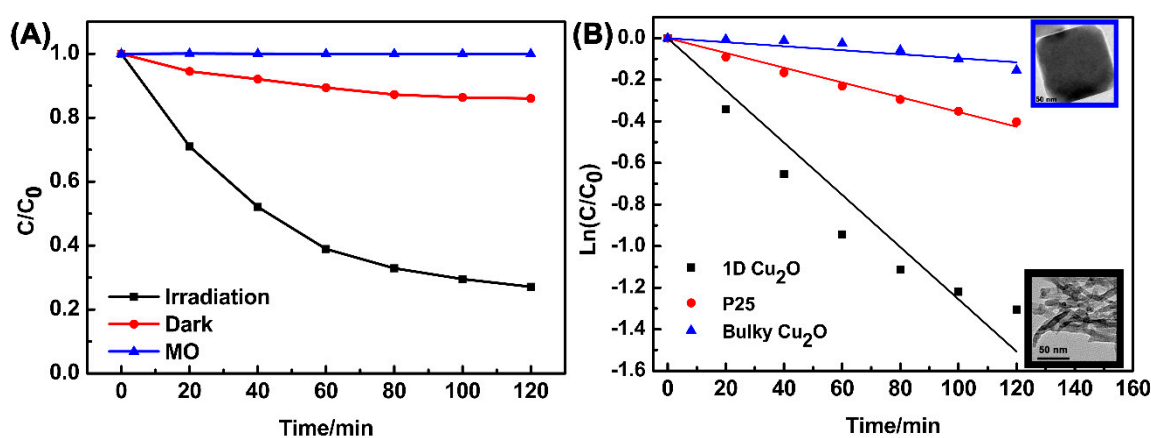


**Figure 6.** Photocatalytic degradation of methyl orange (MO) versus visible light irradiation duration by  $\text{Cu}_2\text{O}$  (A); the kinetics of MO degradation using various photocatalysts (B).

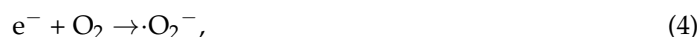
To further study the photocatalytic activity of the as-prepared catalyst, the Langmuir-Hinshelwood model was applied. The pseudo-first-order kinetic equation:  $-\ln(C/C_0^{-1}) = kt$  was used to describe the reaction kinetics, where  $k$  is the kinetic constant. The higher rate constant  $k$  indicates the faster degradation rate [43]. As shown in Figure 6B, the MO photodegradation was in accordance with pseudo-first-order kinetics. The kinetic constants ( $k$ ) and regression coefficients ( $R^2$ ) listed in Table 1 were obtained from the simulated straight lines in the plot of  $\ln(C/C_0^{-1})$  versus time. The prepared  $\text{Cu}_2\text{O}$  presented much better photocatalytic performance than commercial P25 and bulky  $\text{Cu}_2\text{O}$ , which were 3.5 and 13 times greater, respectively. This could possibly be ascribed to the visible light response and large active site area of the prepared  $\text{Cu}_2\text{O}$ .

**Table 1.** Degradation parameters of kinetic constant ( $k$ ,  $\text{min}^{-1}$ ) and  $R^2$  using different photocatalysts under visible light irradiation.

Sample	Kinetic Constant ( $k$ , $\text{min}^{-1}$ )	$R^2$
One-dimensional $\text{Cu}_2\text{O}$	$1.26 \times 10^{-2}$	0.976
P25	$3.55 \times 10^{-3}$	0.995
Bulky $\text{Cu}_2\text{O}$	$9.64 \times 10^{-4}$	0.877

Generally, photocatalytic degradation starts from the generation of photogenerated electron-hole pairs under light irradiation. The electrons in the valence band can be excited to the conductive band, leaving holes in the valence band. The free electrons in the conductive band can be scavenged by  $\text{O}_2$

and transformed into active  $\cdot\text{O}_2^-$ , and the holes in the valence band can react with  $\text{H}_2\text{O}$  and form  $\cdot\text{OH}$  [44], as shown in the following reactions:



Several reactive intermediate species such as  $\cdot\text{O}_2^-$ , and  $\cdot\text{OH}$ , together with  $h^+$ , are capable of degrading in photocatalytic processes. The role the reactive species plays in the photocatalytic process was explored by a trapping experiment. In the experiment, IPA, TEOA, and L-AA were used as typical scavengers of  $\cdot\text{OH}$ ,  $h^+$  and  $\cdot\text{O}_2^-$ , respectively [45]. As Figure 7 shows, the degradation rates of MO reduced from 73.0% to 64.6%, 9%, and 15%, respectively. In conclusion,  $h^+$  and  $\cdot\text{O}_2^-$  species made the biggest contributions to MO degradation [45]. This result provides us with an insight to improve the photocatalytic ability of the product by suppressing  $h^+$  converting to  $\cdot\text{OH}$ . To accomplish this, an acidic medium should be enough to suppress Reaction (5) and save the holes for degradation. In the meantime, making a composite using a second component in addition to  $\text{Cu}_2\text{O}$  for electron and hole separation is a typical route for photocatalytic improvement.

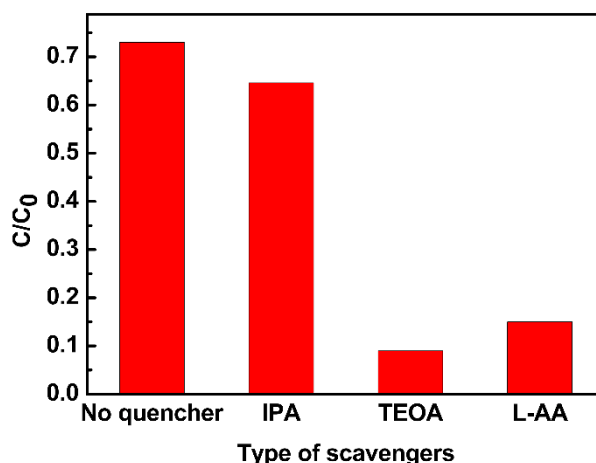


Figure 7. Trapping experiment of the active species.

As for the reusability of the prepared  $\text{Cu}_2\text{O}$  nanowires, we found that the degradation reduced greatly after recycling, and part of  $\text{Cu}_2\text{O}$  was oxidized to  $\text{CuO}$ , according to the XRD result. We assume it was because the prepared small-sized  $\text{Cu}_2\text{O}$  nanowires were unstable in water after a long period of irradiation. Therefore, further research is needed to protect the  $\text{Cu}_2\text{O}$  product for the purpose of recycling and to improve its photocatalytic properties.

#### 4. Conclusions

In this work, we prepared one-dimensional  $\text{Cu}_2\text{O}$  nanowires in an efficient and template-free microwave method. The process is characterized by the short time required and the fact that no inducing agent is used. The successful preparation of  $\text{Cu}_2\text{O}$  was confirmed by XRD, EDS, and HRTEM analyses. The possible synthetic mechanism was studied and hypothesized. The quantity of  $\text{NaOH}$  and the microwave energy were confirmed to work synergistically toward the formation of one-dimensional  $\text{Cu}_2\text{O}$  nanowires. The preferred photocatalytic ability of the prepared sample was examined by degrading MO under visible light at room temperature. The result showed 73% of the MO was removed under visible light irradiation for 120 min with only 4 mg of the prepared catalyst. However, the reuse stability and other applications of the product need further improvement. This research provides a novel method for the preparation of one-dimensional  $\text{Cu}_2\text{O}$

nanowires. We believe this microwave-assisted preparation may provide a green and new ideal for one-dimensional material synthesis.

**Author Contributions:** Conceptualization, R.C. and Z.W.; Methodology, R.C.; Software, R.C.; Validation, R.C., Z.W. and Q.Z.; Formal Analysis, R.C.; Investigation, R.C.; Resources, Z.W.; Data Curation, R.C. and Q.Z.; Writing-Original Draft Preparation, R.C.; Writing-Review & Editing, J.L.; Visualization, R.C.; Supervision, Z.W.; Project Administration, M.Z.; Funding Acquisition, M.Z.

**Funding:** This work was supported by a key project for Industry-Academia-Research in Jiangsu province (BY2016043-01).

**Conflicts of Interest:** The authors declare that they have no conflict of interest.

## References

1. Zhang, W.; Wang, B.; Hao, C.; Liang, Y.; Shi, H.; Ao, L.; Wang, W. Au/Cu<sub>2</sub>O Schottky contact heterostructures with enhanced photocatalytic activity in dye decomposition and photoelectrochemical water splitting under visible light irradiation. *J. Alloys Compd.* **2016**, *684*, 445–452. [[CrossRef](#)]
2. Zhang, Y.; Deng, B.; Zhang, T.; Gao, D.; Xu, A.W. Shape Effects of Cu<sub>2</sub>O Polyhedral Microcrystals on Photocatalytic Activity. *J. Phys. Chem. C* **2010**, *114*, 5073–5079. [[CrossRef](#)]
3. Tadjarodi, A.; Akhavan, O.; Bijanzad, K. Photocatalytic activity of CuO nanoparticles incorporated in mesoporous structure prepared from bis(2-aminonicotinato) copper(II) microflakes. *Trans. Nonferrous Met. Soc. China* **2015**, *25*, 3634–3642. [[CrossRef](#)]
4. Xu, H.; Wang, W.; Zhu, W. Shape Evolution and Size-Controllable Synthesis of Cu<sub>2</sub>O Octahedra and Their Morphology-Dependent Photocatalytic Properties. *J. Phys. Chem. B* **2006**, *110*, 13829–13834. [[CrossRef](#)] [[PubMed](#)]
5. Huang, M.H.; Naresh, G.; Chen, H.S. Facet-Dependent Electrical, Photocatalytic, and Optical Properties of Semiconductor Crystals and Their Implications for Applications. *ACS Appl. Mater. Interfaces* **2017**, *10*, 4–15. [[CrossRef](#)] [[PubMed](#)]
6. Zheng, Z.; Huang, B.; Wang, Z.; Guo, M.; Qin, X.; Zhang, X.; Wang, P.; Dai, Y. Crystal Faces of Cu<sub>2</sub>O and Their Stabilities in Photocatalytic Reactions. *J. Phys. Chem. C* **2009**, *113*, 14448–14453. [[CrossRef](#)]
7. Ma, J.; Guo, S.; Guo, X.; Ge, H. Preparation, characterization and antibacterial activity of core-shell Cu<sub>2</sub>O@Ag composites. *Surf. Coat. Technol.* **2015**, *272*, 268–272. [[CrossRef](#)]
8. Lee, Y.J.; Kim, S.; Park, S.H.; Park, H.; Huh, Y.D. Morphology-dependent antibacterial activities of Cu<sub>2</sub>O. *Mater. Lett.* **2011**, *65*, 818–820. [[CrossRef](#)]
9. Xu, Z.; Ye, S.; Zhang, G.; Li, W.; Gao, C.; Shen, C.; Meng, Q. Antimicrobial polysulfone blended ultrafiltration membranes prepared with Ag/Cu<sub>2</sub>O hybrid nanowires. *J. Membr. Sci.* **2016**, *509*, 83–93. [[CrossRef](#)]
10. Lamberti, A.; Destro, M.; Bianco, S.; Quaglio, M.; Chiodoni, A.; Pirria, C.F.; Gerbaldi, C. Facile fabrication of cuprous oxide nanocomposite anode films for flexible Li-ion batteries via thermal oxidation. *Electrochim. Acta* **2012**, *86*, 323–329. [[CrossRef](#)]
11. Ma, S.; Liu, Q.; Lei, D.; Guo, X.; Li, S.; Li, Z. A powerful LiO<sub>2</sub> battery based on an efficient hollow Cu<sub>2</sub>O cathode catalyst with tailored crystal plane. *Electrochim. Acta* **2018**, *260*, 31–39. [[CrossRef](#)]
12. Chen, W.; Zhang, W.; Chen, L.; Zeng, L.; Wei, M. Facile synthesis of Cu<sub>2</sub>O nanorod arrays on Cu foam as a self-supporting anode material for lithium ion batteries. *J. Alloys Compd.* **2017**, *723*, 172–178. [[CrossRef](#)]
13. Şişman, O.; Kılınç, N.; Öztürk, Z.Z. H<sub>2</sub> Sensing Properties of Cu<sub>2</sub>O Nanowires on Glass Substrate. *Procedia Eng.* **2015**, *120*, 1170–1174. [[CrossRef](#)]
14. Yin, H.; Cui, Z.; Wang, L.; Nie, Q. In situ reduction of the Cu/Cu<sub>2</sub>O/carbon spheres composite for enzymaticless glucose sensors. *Sens. Actuators B-Chem.* **2016**, *222*, 1018–1023. [[CrossRef](#)]
15. Wang, M.; Song, X.; Song, B.; Liu, J.; Hu, C.; Wei, D.; Wong, C.P. Precisely quantified catalyst based on in situ growth of Cu<sub>2</sub>O nanoparticles on a graphene 3D network for highly sensitive glucose sensor. *Sens. Actuators B-Chem.* **2017**, *250*, 333–341. [[CrossRef](#)]
16. He, P.; Shen, X.; Gao, H. Size-controlled preparation of Cu<sub>2</sub>O octahedron nanocrystals and studies on their optical absorption. *J. Colloid Interface Sci.* **2005**, *284*, 510–515. [[CrossRef](#)] [[PubMed](#)]
17. Han, N.; Yang, Z.; Shen, L.; Lin, H.; Wang, Y.; Pun, E.Y.B.; Chen, Y.; Ho, J.C. Design and fabrication of 1-D semiconductor nanomaterials for high-performance photovoltaics. *Sci. Bull.* **2016**, *61*, 357–367. [[CrossRef](#)]

18. Zhou, T.; Zang, Z.; Wei, J.; Zheng, J.; Hao, J.; Ling, F.; Tang, X.; Fang, L.; Zhou, M. Efficient charge carrier separation and excellent visible light photoresponse in Cu<sub>2</sub>O nanowires. *Nano Energy* **2018**, *50*, 118–125. [[CrossRef](#)]
19. Sun, S.; Zhang, X.; Yang, Q.; Liang, S.; Zhang, X.; Yang, Z. Cuprous oxide (Cu<sub>2</sub>O) crystals with tailored architectures: A comprehensive review on synthesis, fundamental properties, functional modifications and applications. *Prog. Mater. Sci.* **2018**, *96*, 111–173. [[CrossRef](#)]
20. Ng, S.Y.; Ngan, A.H.W. One- and two-dimensional cuprous oxide nano/micro structures fabricated on highly orientated pyrolytic graphite (HOPG) by electrodeposition. *Electrochim. Acta* **2013**, *114*, 379–386. [[CrossRef](#)]
21. Wang, W.Z.; Wang, G.H.; Wang, X.S.; Zhan, Y.J.; Liu, Y.K.; Zheng, C.L. Synthesis and Characterization of Cu<sub>2</sub>O Nanowires by a Novel Reduction Route. *Adv. Mater.* **2002**, *14*, 67–69. [[CrossRef](#)]
22. Wang, S.; Huang, Q.; Wen, X.; Li, X.; Yang, S. Thermal oxidation of Cu<sub>2</sub>S nanowires: A template method for the fabrication of mesoscopic Cu<sub>x</sub>O (x = 1,2) wires. *Phys. Chem. Chem. Phys.* **2002**, *4*, 3425–3429. [[CrossRef](#)]
23. Deng, S.; Tjoa, V.; Fan, H.M.; Tan, H.R.; Sayle, D.C.; Olivo, M.; Mhaisalkar, S.; Wei, J.; Sow, C.H. Reduced Graphene Oxide Conjugated Cu<sub>2</sub>O Nanowire Mesocrystals for High-Performance NO<sub>2</sub> Gas Sensor. *J. Am. Chem. Soc.* **2012**, *134*, 4905–4917. [[CrossRef](#)] [[PubMed](#)]
24. Wen, X.; Xie, Y.; Choi, C.L.; Wan, K.C.; Li, X.Y.; Yang, S. Copper-Based Nanowire Materials: Templated Syntheses, Characterizations, and Applications. *Langmuir* **2005**, *21*, 4729–4737. [[CrossRef](#)] [[PubMed](#)]
25. Nunes, D.; Pimentel, A.; Barquinha, P.; Carvalho, P.A.; Fortunato, E.; Martins, R. Cu<sub>2</sub>O polyhedral nanowires produced by microwave irradiation. *J. Phys. Chem. C* **2014**, *2*, 6097–6103. [[CrossRef](#)]
26. Nunes, D.; Calmeiro, T.R.; Nandy, S.; Pinto, J.V.; Pimentel, A.; Barquinha, P.; Carvalho, P.A.; Walmsley, J.C.; Fortunato, E.; Martins, R. Charging effects and surface potential variations of Cu-based nanowires. *Thin Solid Films* **2016**, *601*, 45–53. [[CrossRef](#)]
27. Tan, Y.; Xue, X.; Peng, Q.; Zhao, H.; Wang, H.; Li, Y. Controllable Fabrication and Electrical Performance of Single Crystalline Cu<sub>2</sub>O Nanowires with High Aspect Ratios. *Nano Lett.* **2007**, *7*, 3723–3728. [[CrossRef](#)]
28. Xiong, Y.; Li, Z.; Zhang, R.; Xie, Y.; Yang, J.; Wu, C. From Complex Chains to 1D Metal Oxides: A Novel Strategy to Cu<sub>2</sub>O Nanowires. *J. Phys. Chem. B* **2003**, *107*, 3697–3702. [[CrossRef](#)]
29. Orel, Z.C.; Anžlovar, A.; Dražič, G.; Žigon, M. Cuprous Oxide Nanowires Prepared by an Additive-Free Polyol Process. *Cryst. Growth Des.* **2007**, *7*, 453–458. [[CrossRef](#)]
30. Li, C.W.; Kanan, M.W. CO<sub>2</sub> reduction at low overpotential on Cu electrodes resulting from the reduction of thick Cu<sub>2</sub>O films. *J. Am. Chem. Soc.* **2012**, *134*, 7231–7234. [[CrossRef](#)] [[PubMed](#)]
31. Liu, X.; Hu, R.; Xiong, S.; Liu, Y.; Chai, L.; Bao, K.; Qian, Y. Well-aligned Cu<sub>2</sub>O nanowire arrays prepared by an ethylene glycol-reduced process. *Mater. Chem. Phys.* **2009**, *114*, 213–216. [[CrossRef](#)]
32. Bhosale, M.A.; Bhatte, K.D.; Bhanage, B.M. A rapid, one pot microwave assisted synthesis of nanosize cuprous oxide. *Powder Technol.* **2013**, *235*, 516–519. [[CrossRef](#)]
33. Liu, F.K.; Huang, P.W.; Chang, Y.C.; Ko, C.J.; Ko, F.H.; Chu, T.C. Formation of silver nanorods by microwave heating in the presence of gold seeds. *J. Cryst. Growth* **2005**, *273*, 439–445. [[CrossRef](#)]
34. Bhatte, K.D.; Tambade, P.; Fujita, S.; Arai, M.; Bhanage, B.M. Microwave-assisted additive free synthesis of nanocrystalline zinc oxide. *Powder Technol.* **2010**, *203*, 415–418. [[CrossRef](#)]
35. Bhatte, K.D.; Sawant, D.N.; Deshmukh, K.M.; Bhanage, B.M. Additive free microwave assisted synthesis of nanocrystalline Mg(OH)<sub>2</sub> and MgO. *Particuology* **2012**, *10*, 384–387. [[CrossRef](#)]
36. Zhang, H.; Liu, F.; Li, B.; Xu, J.; Zhao, X.; Liu, X. Microwave-assisted synthesis of Cu<sub>2</sub>O microcrystals with systematic shape evolution from octahedral to cubic and their comparative photocatalytic activities. *RSC Adv.* **2014**, *4*, 38059–38063. [[CrossRef](#)]
37. Zou, X.; Fan, H.; Tian, Y.; Zhang, M.; Yan, X. Microwave-assisted hydrothermal synthesis of Cu/Cu<sub>2</sub>O hollow spheres with enhanced photocatalytic and gas sensing activities at room temperature. *Dalton Trans.* **2015**, *44*, 7811–7821. [[CrossRef](#)] [[PubMed](#)]
38. Luévano-Hipólito, E.; Torres-Martínez, L.M.; Sánchez-Martínez, D.; Alfaro Cruz, M.R. Cu<sub>2</sub>O precipitation-assisted with ultrasound and microwave radiation for photocatalytic hydrogen production. *Int. J. Hydrogen Energy* **2017**, *42*, 12997–13010. [[CrossRef](#)]
39. Pimentel, A.; Nunes, D.; Duarte, P.; Rodrigues, J.; Costa, F.M.; Monteiro, T.; Martins, R.; Fortunato, E. Synthesis of Long ZnO Nanorods under Microwave Irradiation or Conventional Heating. *J. Phys. Chem. C* **2014**, *118*, 14629–14639. [[CrossRef](#)]

40. Chen, R.; Lu, J.; Wang, Z.; Zhou, Q.; Zheng, M. Microwave Synthesis of Cu/Cu<sub>2</sub>O/SnO<sub>2</sub> Composite with Improved Photocatalytic Ability Using SnCl<sub>4</sub> as a Protector. *J. Mater. Sci.* **2018**, *53*, 9557–9566. [[CrossRef](#)]
41. Cheng, Z.; Xu, J.; Zhong, H.; Chu, X.Z.; Song, J. Repeatable synthesis of Cu<sub>2</sub>O nanorods by a simple and novel reduction route. *Mater. Lett.* **2011**, *65*, 1871–1874. [[CrossRef](#)]
42. Pimentel, A.; Rodrigues, J.; Duarte, P.; Nunes, D.; Costa, F.M.; Monteiro, T.; Martins, R.; Fortunato, E. Effect of solvents on ZnO nanostructures synthesized by solvothermal method assisted by microwave radiation: A photocatalytic study. *J. Mater. Sci.* **2015**, *50*, 5777–5787. [[CrossRef](#)]
43. Luo, Y.; Huang, Q.; Li, B.; Dong, L.; Fan, M.; Zhang, F. Synthesis and characterization of Cu<sub>2</sub>O-modified Bi<sub>2</sub>O<sub>3</sub> nanospheres with enhanced visible light photocatalytic activity. *Appl. Surf. Sci.* **2015**, *357*, 1072–1079. [[CrossRef](#)]
44. Zhou, Z.; Long, M.; Cai, W.; Cai, J. Synthesis and photocatalytic performance of the efficient visible light photocatalyst Ag–AgCl/BiVO<sub>4</sub>. *J. Mol. Catal. A-Chem.* **2012**, *353–354*, 22–28. [[CrossRef](#)]
45. Liu, S.; Zheng, M.; Chen, R.; Wang, Z. One-pot synthesis of an AgBr/ZnO hierarchical structure with enhanced photocatalytic capacity. *RSC Adv.* **2017**, *7*, 31230–31238. [[CrossRef](#)]



© 2018 by the authors. Licensee MDPI, Basel, Switzerland. This article is an open access article distributed under the terms and conditions of the Creative Commons Attribution (CC BY) license (<http://creativecommons.org/licenses/by/4.0/>).